

Comparision of Physical Properties of Different Compositions of Alumina/Lanthanum Hexaaluminate Ceramic Composite

**A THESIS SUBMITTED IN PARTIAL FULLFILLMENT OF THE REQUIREMENTS
FOR THE DEGREE OF BACHELOR OF TECHNOLOGY**

By

ROHIT MOHAPATRA



DEPARTMENT OF CERAMIC ENGINEERING

NATIONAL INSTITUTE OF TECHNOLOGY

ROURKELA

2009-2010

Comparision of Physical Properties of Different Compositions of Alumina/Lanthanum Hexaaluminate Ceramic Composite

**A THESIS SUBMITTED IN PARTIAL FULLFILLMENT OF THE REQUIREMENTS
FOR THE DEGREE OF BACHELOR OF TECHNOLOGY**

By

ROHIT MOHAPATRA

(10608014)

Under the Guidance of

Prof. Swadesh Kumar Pratihar



DEPARTMENT OF CERAMIC ENGINEERING

NATIONAL INSTITUTE OF TECHNOLOGY

ROURKELA

2009-2010



National Institute of Technology Rourkela

CERTIFICATE

This is to certify that the project entitled, **“COMPARISION OF PHYSICAL PROPERTIES OF DIFFERENT COMPOSITIONS OF ALUMINA/LANTHANUM HEXAALUMINATE CERAMIC COMPOSITE”** submitted by **Rohit Mohapatra** is an authentic work carried out by him under my supervision and guidance for the partial fulfillment of the requirements for the award of **Bachelor of Technology Degree in Ceramic Engineering** at **National Institute of Technology, Rourkela.**

To the best of my knowledge, the matter embodied in the project has not been submitted to any other University / Institute for the award of any Degree or Diploma.

Date- 07/05/2010

Rourkela

(Prof. Swadesh Kumar Pratihar)

**Dept. of Ceramic Engineering
NIT Rourkela.**

ACKNOWLEDGEMENT

I wish to express my deep sense of gratitude and indebtedness to Prof. Swadesh K. Pratihara, Department of Ceramic Engineering, NIT Rourkela for introducing the present topic and for his inspiring guidance, constructive criticism and valuable suggestion throughout this project work.

My heartfelt thanks to all the faculty members and staff members of Department of Ceramic Engineering, NIT Rourkela for their suggestions and help during this project work.

I am also thankful to Mr. Sanjay Kumar Swain and other research scholars in Department of Ceramic Engineering for providing all joyful environment in the lab and helping me out in different ways.

I feel a deep sense of gratitude for my father Dr. R.K. Mohapatra, mother Mrs. Rita Mohapatra and brother Romit Mohapatra who formed a part of my vision and taught me the good things that really matter in life.

Last but not least, my sincere thanks to all my friends who have patiently extended all sorts of help for accomplishing this undertaking.

Rohit Mohapatra

10608014

(7th May 2010)

ABSTRACT

The aim of this study was to prepare four different composition of Alumina/Lanthanum Hexaaluminate powder. Four different compositions ranging from 10 to 80 vol % of Lanthanum Hexaaluminate were prepared. To prepare the Alumina-Lanthanum Hexaaluminate ceramic composite, stable aqueous Alumina slurry was needed to prepare. Thus, selection of electrolyte was made after comparing Darvan and tri-ammonium Cytrate. Darvan was chosen as an electrolyte to prepare stable aqueous Alumina slurry. The effect of pH on zeta potential was also studied.

After preparation of Alumina-Lanthanum Hexaaluminate ceramic composite powder, pellets of approximately 0.7gram for each composition were made by applying 4 Ton pressure for 120 seconds. The pellets were then sintered at 1650⁰C in chamber furnace. The soaking time was kept for 4 hours. Then the bulk density, aparent porosity and strength were compared after calculation of dry weight, soked weight, suspended weight. The results revealed that bulk density increased with increasing vol % of LHA content and aparent porosity decreased with increasing vol% of LHA content. The strength also increased with increasing vol% of Lanthanum Hexaaluminate.

LIST OF FIGURES

FIGURE NO.	NAME OF THE FIGURE	PAGE NO.
1.1	Alumina crystal structure	15
1.2	Schematic drawing of the cation attraction on alpha-alumina particles by electrostatic interactions	17
3	Flow chart for preparation of pellets	28
4.1	Zeta Potential v/s pH curve for an aqueous alumina slurry without any addition of electrolyte or dispersant.	35
4.2	Zeta Potential v/s pH curve for aqueous alumina slurry with addition of 0.04 wt. % tri-ammonium cytrate.	36
4.3	Zeta Potential v/s pH curve for aqueous alumina slurry with addition of 0.035wt. % Darvan	37
4.4	Table containing the dry wt., suspended wt., soaked wt., bulk density, aparent porosity and strength of pellets with different composition.	38
4.5	Bulk density curve obtained for pellets of different composition.	39
4.6	Bulk density bar for different pellets with composition containing 10 vol %, 20 vol %, 40 vol % and vol% LHA.	40
4.7	Aparent porosity curve obtained for pellets of different composition.	41
4.8	Aparent porosity bar for	42

	different pellets with composition containing 10 vol%, 20 vol %, 40 vol % and vol% LHA.	
4.9	Strength bar for different pellets with composition containing 10 vol%, 20 vol %, 40 vol % and vol% LHA.	43
4.10	Strength curve for different pellets with composition containing 10 vol%, 20 vol %, 40 vol % and vol% LHA.	44

CONTENTS	PAGE NO
ABSTRACT	5
1. INTRODUCTION	10
1.1 CERAMIC COMPOSITES	11
1.1.1 Physical Properties	11
1.1.2 Uses and Applications	11
1.2 WHY $\text{Al}_2\text{O}_3 - x \text{LaAl}_{11}\text{O}_{18}$?	12
1.3 ALUMINIUM OXIDE	13
1.3.1 Natural Occurrence	14
1.3.2 Properties	14
1.3.3 Typical Characteristics	15
1.3.4 Crystal Structure	15
1.3.6 Typical Uses	16
1.4 ZETA POTENTIAL	17
1.4.1 Zeta Potential and pH	18
2. LITERATURE REVIEW	20
2.1 Effect of pH, Temperature and concentration of electrolyte in Zeta Potential.	21
2.2 Preparation of $\text{Al}_2\text{O}_3/\text{LHA}$ Ceramic Composite	24
2.3 OBJECTIVE OF THE PRESENT STUDIES	26
3. EXPERIMENTAL PROCEDURE	27
3.1 PREPARATION OF 0.2M AMMONIUM CARBONATE SOLUTION	29
3.2 PREPARATION OF $\text{Al}_2\text{O}_3 - x \text{LaAl}_{11}\text{O}_{18}$ POWDER.	29

3.2.1 Al ₂ O ₃ – 10 LaAl ₁₁ O ₁₈ Powder	29
3.2.2 Al ₂ O ₃ – 20 LaAl ₁₁ O ₁₈ Powder	30
3.2.3 Al ₂ O ₃ – 40 LaAl ₁₁ O ₁₈ Powder	31
3.2.4 Al ₂ O ₃ – 80 LaAl ₁₁ O ₁₈ Powder	32
4. RESULTS AND DISCUSSION	34
4.1 Zeta Potential without addition of Electrolyte/Dispersant	35
4.2 Zeta Potential with addition of Dispersant	36
4.3 Zeta Potential with addition of Electrolyte	37
4.4 Table I	38
4.5 Bulk Density plot for different composition of LHA(Graph I)	39
4.6 Bulk Density plot for different composition of LHA(Graph II)	40
4.7 Aparent Density plot for different composition of LHA(Graph I)	41
4.8 Aparent Density plot for different composition of LHA(Graph II)	42
4.9 Bar Chart for Strength of Pellets for different composition of LHA	43
4.10 Strength Curve of Pellets for different composition of LHA	44
5. CONCLUSION	45
6. REFERENCES	46

CHAPTER - 1

INTRODUCTION

1.1 CERAMIC COMPOSITES

Composite materials are engineered materials made from two or more constituent materials with significantly different physical or chemical properties which remain separate and distinct on a macroscopic level within the finished structure.[11]

1.1.1 Physical Properties

The physical properties of composite materials are generally not isotropic (independent of direction of applied force) in nature, but rather are typically orthotropic (different depending on the direction of the applied force or load). For instance, the stiffness of a composite panel will often depend upon the orientation of the applied forces and/or moments. Panel stiffness is also dependent on the design of the panel. For instance, the fiber reinforcement and matrix used the method of panel build, thermoset versus thermoplastic, type of weave, and orientation of fiber axis to the primary force.[11]

1.1.2 Uses and Applications

Composite materials have gained popularity (despite their generally high cost) in high-performance products that need to be lightweight, yet strong enough to take harsh loading conditions such as aerospace components (tails, wings, fuselages, propellers), boat and scull hulls, bicycle frames and racing car bodies. Other uses include fishing rods, storage tanks, and baseball bats. The new Boeing 787 structure including the wings and fuselage is composed

largely of composites. Composite materials are also becoming more common in the realm of orthopedic surgery.

Carbon composite is a key material in today's launch vehicles and spacecraft. It is widely used in solar panel substrates, antenna reflectors and yokes of spacecraft. It is also used in payload adapters, inter-stage structures and heat shields of launch vehicles.[11]

1.2 WHY $\text{Al}_2\text{O}_3 - x \text{LaAl}_{11}\text{O}_{18}$?

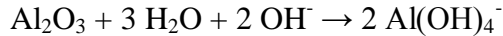
Ceramic composites have attracted attention for the development of desired materials required for space, terrestrial, energetic, and many other applications due to their light weight, high mechanical strength and fracture toughness, high temperature capabilities, low thermal expansion, high abrasive resistance, and graceful failure under loading. Much effort has been spent on the advancement of non-oxide ceramic composites, but most of the superior mechanical properties of these composites can only be of benefit if they are used in inert atmospheres. Therefore, the possible breakthrough of oxide/oxide ceramic composites with long-time stability at high temperatures even in oxidising atmospheres has attracted much more attention recently. The properties of oxide-based ceramic composites are strongly dependent on the microstructure characteristics, e.g., the size and shape of grains, the amount of porosity and the pore size, the distribution of pores in the body, and the nature and distribution of any second phases. Hence, the important key for obtaining the desired properties is designing the microstructure via processing. There is a growing interest in the development of particulate composites with microstructures exhibiting plate-like morphologies in the processing point of view, as well as in porous composite ceramics with pore morphological and thermochemical stability and desired

thermophysical properties for applications at elevated temperatures. Lanthanum hexaaluminate (LHA) with an ideal stoichiometry $\text{LaAl}_{11}\text{O}_{18}$, and a platelet-like morphology is a candidate material for adjustment of the fibre-matrix interfaces, reinforcement of the particulate composites, and then applications in high-temperature thermal barrier coatings.[7] [8] [9] [10]

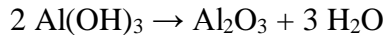
1.3 ALUMINIUM OXIDE

Aluminium oxide is an amphoteric oxide of aluminium with the chemical formula Al_2O_3 . It is also commonly referred to as **alumina** or **aloxite** in the mining, ceramic and materials science communities. It is produced by the Bayer process from bauxite.

Bauxite is purified by the Bayer Process:



The other components of bauxite do not dissolve. The SiO_2 dissolves as silicate $\text{Si}(\text{OH})_6^{2-}$. Upon filtering, Fe_2O_3 is removed. When the Bayer liquor is cooled, $\text{Al}(\text{OH})_3$ precipitates, leaving the silicates in solution. The mixture is then calcined to give aluminium oxide:



The formed Al_2O_3 is alumina. The alumina formed tends to be multi-phase; i.e., constituting several of the alumina phases rather than solely corundum. The production process can therefore be optimized to produce a tailored product. The type of phases present affects, for example, the solubility and pore structure of the alumina product which, in turn, affects the cost of aluminium production and pollution control.

Its most significant use is in the production of aluminium metal, although it is also used as an abrasive due to its hardness and as a refractory material due to its high melting point.

1.3.1 Natural Occurrence

The naturally occurring crystalline form of aluminium oxide is Corundum. The gem-quality forms of corundum are Rubies and Sapphires. Due to trace impurities in the corundum structure, they have their characteristic colors.

1.3.2 Properties

Aluminium oxide has a relatively high thermal conductivity (40 W/m K) but is an electrical insulator. The hardness of alpha-alumina makes it suitable for use as an abrasive and as a component in cutting tools.

Aluminium oxide is responsible for metallic aluminium's resistance to weathering. Metallic aluminium is very reactive with atmospheric oxygen, and a thin passivation layer of alumina quickly forms on any exposed aluminium surface. This layer protects the metal from further oxidation. Anodising is used to enhance the thickness and properties of this oxide layer. By including a proportion of aluminium in the alloy, a number of alloys, such as aluminium bronzes, exploit this property to enhance corrosion resistance. The alumina generated by anodising is typically amorphous, but discharge assisted oxidation processes such as plasma electrolytic oxidation result in a significant proportion of crystalline alumina in the coating, enhancing its hardness.

1.3.3 Typical Characteristics

- > Good strength and Stiffness.
- > Good hardness and wear.
- > Good corrosion resistance.
- > Good thermal stability.
- > Excellent dielectric properties.
- > Low dielectric constant.
- > Low loss tangent.

1.3.4 Crystal Structure

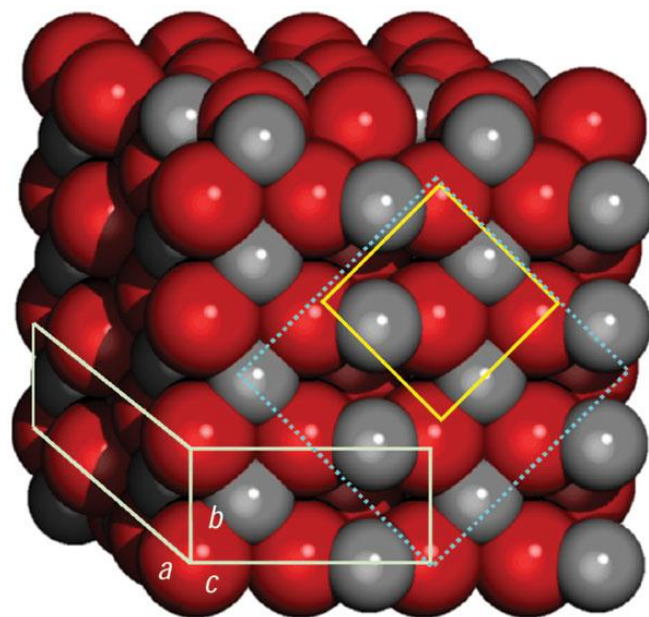


Fig 1.1: Schematic diagram showing Alumina crystal structure.

Aluminium atoms are arranged in a fcc structure. Aluminium has stacking fault energy of approximately 200 mJ/m^2 . Corundum has a trigonal Bravais lattice. Each unit cell contains six formula units of aluminium oxide. The oxygen ions nearly form a hexagonal close-packed structure with aluminium ions filling two-thirds of the octahedral interstices.

1.3.6 Typical Uses

- > Seal rings.
- > Medical prostheses.
- > Laser tubes.
- > Electronic substrates.
- > Ballistic armour.
- > Thermocouple tubes.
- > Grinding media.
- > Wear components.

1.4 ZETA POTENTIAL

Colloidal particles dispersed in a solution are electrically charged due to their ionic characteristics and dipolar attributes. Each particle dispersed in a solution is surrounded by oppositely charged ions called the fixed layer. Outside the fixed layer, there are varying compositions of ions of opposite polarities, forming a cloud-like area. This area is called the diffuse double layer, and the whole area is electrically neutral.

When a voltage is applied to the solution in which particles are dispersed, particles are attracted to the electrode of the opposite polarity, accompanied by the fixed layer and part of the diffuse double layer, or internal side of the "sliding surface". Zeta potential is considered to be the electric potential of this inner area including this conceptual "sliding surface". As this electric potential approaches zero, particles tend to aggregate.

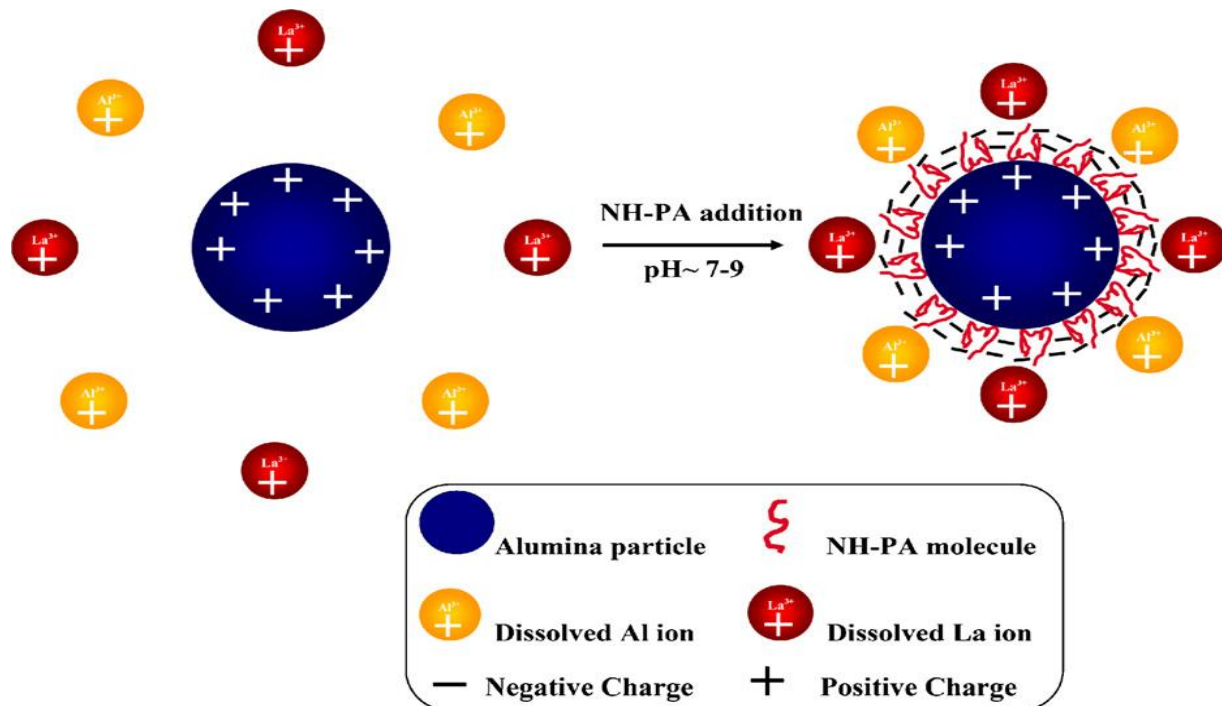


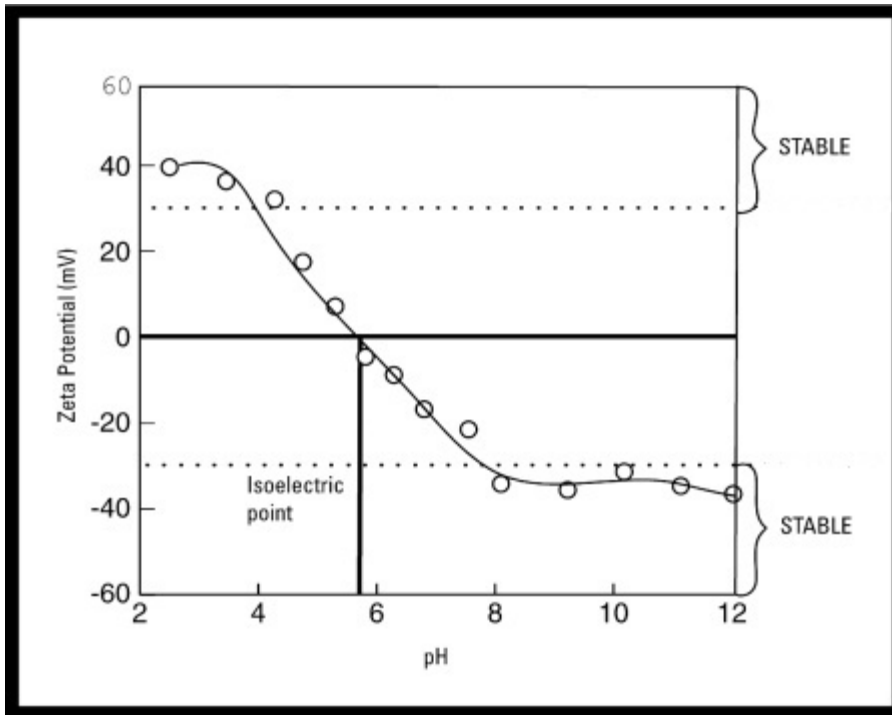
Fig 1.2: Schematic drawing of the cation attraction on alpha-alumina particles by electrostatic interactions.[10]

1.4.1 Zeta Potential and pH

The most important factor that affects zeta potential is pH. A zeta potential value quoted without a definition of its environment (pH, ionic strength, concentration of any additives) is a meaningless number.

Imagine a particle in suspension with a negative zeta potential

- If more alkali is added to this suspension then the particles tend to acquire more negative charge
- If acid is added to this suspension then a point will be reached where the charge will be neutralized
- Further addition of acid will cause a build up of positive charge
- In general, a zeta potential versus pH curve will be positive at low pH and lower or negative at high pH
- There may be a point where the curve passes through zero zeta potential
- This point is called the isoelectric point and is very important from a practical consideration
- It is normally the point where the colloidal system is least stable



In the above example it can be seen that if the dispersion pH is below 4 or above 8 there is sufficient charge to confer stability. However if the pH of the system is between 4 and 8 the dispersion may be unstable. This is most likely to be the case at around pH 6 (the isoelectric point).

CHAPTER – 2
LITERATURE
REVIEW

2.1 Effect of pH, Temperature and concentration of electrolyte in Zeta Potential.

S. Baklouti, C. Pagnoux, T. Chartier & J. F. Baumard successfully processed homogenous and stable Al_2O_3 -SiC mixed slurry to prepare nanocomposites. A new polyelectrolyte was developed (ionized PEI) in order to disperse acidic SiO_2 powder. The same polyelectrolyte was used for dispersion of SiC powder in an aqueous medium where SiC particles were covered with an oxidized layer [1]

R. Ramachandra Rao, H. N. Roopa and T. S. Kannan observed the dispersing behaviour of silicon, silicon carbide and their mixtures in aqueous media which were monitored by particle size, sedimentation, viscosity and zeta potential analyses as a function of pH of the slurry. The pH values for optimum dispersion were found to be 4 and 8 for silicon, 10 for SiC and 9 for Si - SiC mixtures. Optimum slips of Si+SiC mixtures were slip cast to obtain green compacts which were nitrided once at 1450 °C for 2 or 4 h or successively and cumulatively for 8 (2+6) and 10 (4+6) h in a resistively heated graphite furnace. The binding phases in the nitrided products were found to be fibrous/needle like α - Si_3N_4 , flaky grains of β - Si_3N_4 and Si_2ON_2 . The products containing 19 - 47% of silicon nitride as bond/matrix possessed flexural strength (three-point bending) values of 50 - 85 MPa.[2]

Xinwen Zhu, Dongliang Jiang, Shouhong Tan produced reticulated porous ceramics. In this work commercial polyurethane sponge with open porosity of approximately 13 pores per inch were chosen as the templates to produce the SiC reticulated porous ceramics. Effects of the rheological behaviour of the slurry on the coating quality and the properties of the SiC reticulated porous ceramics such as strength, density, microstructure were investigated in detail. The coating quality was found to depend strongly on the slurry viscosity and this was improved dramatically extremely as the viscosity increased. The SiC reticulated porous ceramics displayed a remarkable increase in the flexural strength as the solids content increased. In addition, the increase of the polymer content had also a little contribution to the improvement of the strength. The optimum solids content and polymer content were found to be 80 and 0.2 wt. %.[3]

Pang Xueman, Xu Mingxia, Liang Hui, Li Xiaolei, Ji Huiming investigated the influences of solids concentration, concentration of dispersant and high-speed dispersing time on the rheological behavior of silicon slurries. The effect of poly(acrylic acid) ammonium (PAA-NH₄) dispersant on high solids content silicon suspensions was rheologically characterized. The viscosity and fluidity exhibited a strong dependence on the solids concentration, but when subjected to certain amount of dispersant PAA-NH₄ adsorption and high speed shear sweep investigations, the suspensions demonstrated shear-thinning and thixotropic behavior as a result of changes to the suspension microstructure. Zeta potential and sedimentation character showed that the dispersant was adsorbed on silicon for efficient stabilization at high solids loadings. A general structural kinetics model was presented to describe the flow behavior of the thixotropic

systems. The effect of shear on structure breakdown and build-up, as well as the effect of Brownian motion on build-up were taken into account to the kinetic equation for the structure parameter. Due to the PAA-NH₄ absorption modality, thixotropic model characterized the PAA-NH₄ concentration-dependent behavior of the suspensions over a wide range of PAA-NH₄ concentration.[4]

F.S. Ortega, R.H.R. Castro, D. Gouvea, V.C. Pandolfelli investigated the rheological behavior by changing the concentrations of dispersant (ammonium polyacrylate) and monomers in the suspensions. The zeta potential of alumina suspensions containing each of the different monomers was measured as a function of dispersant additions. The suspension rheological behavior varied significantly depending on the monomer type, which could be explained in terms of repulsive forces, pH changes and additive interactions.[5]

P.C. KAPUR manufactured and studied the properties and usage of a spectrum of low to high temperature thermal insulations and insulating refractories that can be made from rice husk ash, namely: (i) Calcium ferrite bonded porous silica refractory: (ii) Sodium silicate bonded porous silica refractory: (iii) Fired and chemically bonded forsterite Insulating refractory: (iv) Hydraulic setting calcium.[6]

2.2 Preparation of Al₂O₃/LHA Ceramic Composite

Zahra Negahdari, Monika Willert-Porada modified the microstructure and adjusted the porosity in alumina/lanthanum hexaaluminate particulate composites, by altering the lanthanum hexaaluminate content, for the further development of new materials that can be applied in several technological processes. The amount of lanthanum hexaaluminate was varied from 2.8 to 80 vol. % in particulate composites. As a novel approach to develop homogeneously distributed dense and porous alumina/lanthanum hexaaluminate particulate composites, a carbonate coprecipitation method was applied to produce lanthanum aluminate-coated alumina particles. For the coating process itself, a surface charge adjustment called ‘electrostatic attraction’ was utilised. Subsequent reactive sintering of the calcined-coated particles caused the in situ formation of lanthanum hexaaluminate platelets inside the alumina matrix. The prepared composite powders, as well as the sintered samples, were characterised by FE-SEM, TEM, XRD, dilatometry, and mercury porosimetry. The results revealed that the uniform distribution of the low amount of lanthanum hexaaluminate prohibited the grain growth of alumina matrix and resulted in denser microstructures, whereas the increase in the lanthanum hexaaluminate content yielded more porous microstructures.[10]

N. Iyi, Z. Inoue, S. Takekawa and S. Kimura accomplished the least-square refinement of lanthanum hexaaluminate (La_{0.827}Al_{11.9}O_{19.09}) using single crystal X-ray diffraction data. The result of the final anisotropic refinement, corresponding to an *R*-value of 0.039, revealed the structure of a magnetoplumbite type. In the structure interstitial Al ions were found, which were

probably formed by a Frenkel defect mechanism. These interstitial Al ions are proposed to be situated in pairs making a bridge between spinel blocks, and to cause Al and La defects in the intermediate layer ($z = 0.25$). The nonstoichiometry of lanthanum hexaaluminate was attributed to these defects. [8]

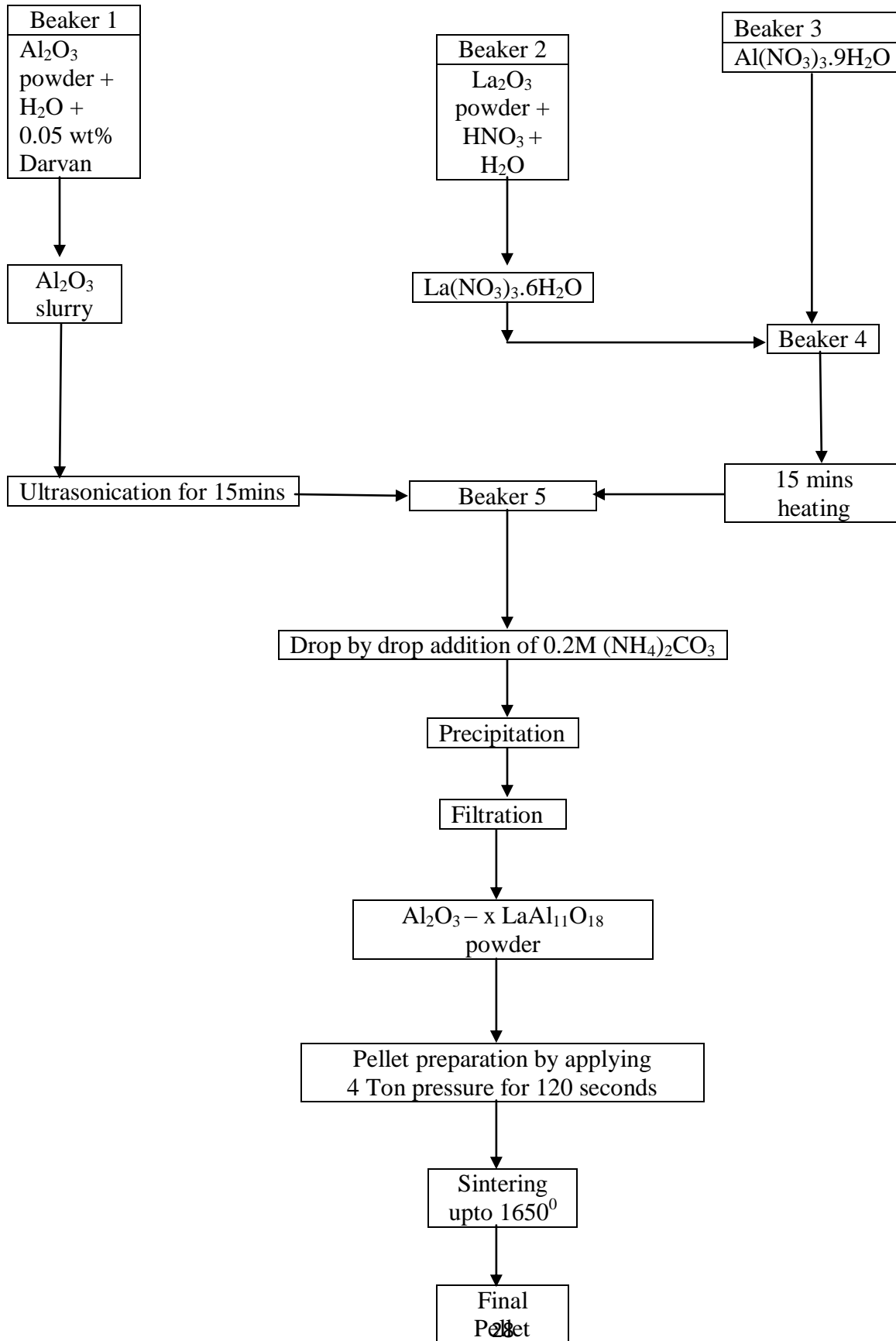
C. Friedrich, R. Gadow and T. Schirmer presented lanthanum hexaaluminate, as a newly developed TBC material with long-term stability up to 1400 °C. It aged significantly more slowly at high temperatures than commercial zirconia-based TBCs. Its composition favored the formation of platelets, which prevented a densification of the coating by postsintering. It consisted of La_2O_3 , Al_2O_3 , and MgO. Its crystal structure corresponded to a magnetoplumbite phase. Lanthanum hexaaluminate powders were produced using two different fabrication routes, one based on salts and the other one based on oxides. To optimize granulate, various raw materials and additives were tested. The slurry was spray dried in a laboratory spray drier and calcined at 1650 °C. Using these two powders, coatings were produced by atmospheric plasma spraying (APS). The residual stresses of the coatings were measured by the hole drilling method, and the deposition process was optimized with respect to the residual stresses in the TBC. The coatings were extensively analyzed regarding phase composition, thermal expansion, and long-term stability, as well as microstructural properties. [7]

2.3 OBJECTIVE OF THE PRESENT STUDIES

- To study the effect of dispersant/electrolyte on aqueous alumina slurry and chose an electrolyte.
- To prepare a stable aqueous alumina slurry and prepare four diferent composition of Alumina-Lanthanum Hexaaluminate composite powder.
- To make pellets of each composition and compare their physical properties.

CHAPTER 3: EXPERIMENTAL PROCEDURE

FLOW CHART FOR PREPARATION OF PELLETS



3.1 PREPARATION OF 0.2M AMMONIUM CARBONATE SOLUTION

Formula Applied

$$M = (W/MM) * (1000/ V_{(\text{in mL})})$$

Molecular Mass of $(\text{NH}_4)_2\text{CO}_3$ or Ammonium Carbonate is 157.13 gms.

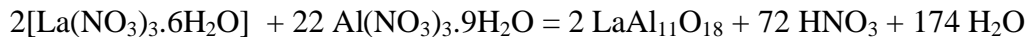
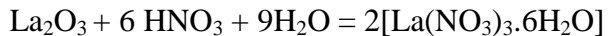
Now,

$$0.2 = (W/157.13) * (1000/250)$$

$$\text{Or } W = 7.8565 \text{ gms.}$$

A measuring cylindrical flask of 250 mL was taken and was filled with 250 mL of distilled water. 7.8565 g of $(\text{NH}_4)_2\text{CO}_3$ was weighed in a butter paper. The measured amount of Ammonium Carbonate was put in the measuring cylindrical flask. The solution was shaken vigorously and a solution of 0.2M Ammonium Carbonate was prepared. [10]

3.2 PREPARATION OF $\text{Al}_2\text{O}_3 - x \text{LaAl}_{11}\text{O}_{18}$ POWDER.



3.2.1 $\text{Al}_2\text{O}_3 - 10 \text{LaAl}_{11}\text{O}_{18}$ POWDER

8.966 g of Alumina powder was taken in a beaker (say beaker 1) containing distilled water. 0.05 wt% Darvan was also added to form stable solution. The solution was put in ultrasonication for fifteen minutes.

0.22 grams of Lanthanum Oxide powder was taken in a butter paper and was put in a beaker (say beaker 2) containing required amount of distilled water. 0.26 grams of Nitric Acid was added to form Lanthanum Nitrate. The solution was stirred continuously and heated for fifteen minutes.

5.88 grams of Aluminium Nitrate was weighed and put in beaker 2. The solution was again stirred and heated for another fifteen minutes.

Both the solutions were mixed and the solution was reheated for fifteen minutes followed by ultrasonication for another fifteen minutes.

0.2 M Ammonium Carbonate Solution was added drop by drop to the solution to form precipitation and then filtration was done using a Wattman 41 filter paper.

The filter paper was allowed to dry overnight and powder of $\text{Al}_2\text{O}_3 - 10 \text{LaAl}_{11}\text{O}_{18}$ were collected.

The ultrasonication was done using Ultrasonic Vibratometer.

3.2.2 $\text{Al}_2\text{O}_3 - 20 \text{LaAl}_{11}\text{O}_{18}$ POWDER

7.926 g of Alumina powder was taken in a beaker (say beaker 1) containing distilled water. 0.05 wt% Darvan was also added to form stable solution. The solution was put in ultrasonication for fifteen minutes.

0.467 grams of Lanthanum Oxide powder was taken in a butter paper and was put in a beaker (say beaker 2) containing required amount of distilled water. 0.54 grams of Nitric Acid was added to form Lanthanum Nitrate. The solution was stirred continuously and heated for fifteen minutes.

11.81 grams of Aluminium Nitrate was weighed and put in beaker 2. The solution was again stirred and heated for another fifteen minutes.

Both the solutions were mixed and the solution was reheated for fifteen minutes followed by ultrasonication for another fifteen minutes.

0.2 M Ammonium Carbonate Solution was added drop by drop to the solution to form precipitation and then filtration was done using a Wattman 41 filter paper.

The filter paper was allowed to dry overnight and powder of $\text{Al}_2\text{O}_3 - 10 \text{LaAl}_{11}\text{O}_{18}$ was collected.

The ultrasonication was done using Ultrasonic Vibratometer.

3.2.3 $\text{Al}_2\text{O}_3 - 40 \text{LaAl}_{11}\text{O}_{18}$ POWDER

5.89 g of Alumina powder was taken in a beaker (say beaker 1) containing distilled water. 0.05 wt% Darvan was also added to form stable solution. The solution was put in ultrasonication for fifteen minutes.

0.92 grams of Lanthanum Oxide powder was taken in a butter paper and was put in a beaker (say beaker 2) containing required amount of distilled water. 1.066 grams of Nitric Acid was added to form Lanthanum Nitrate. The solution was stirred continuously and heated for fifteen minutes.

23.41 grams of Aluminium Nitrate was weighed and put in beaker 2. The solution was again stirred and heated for another fifteen minutes.

Both the solutions were mixed and the solution was reheated for fifteen minutes followed by ultrasonication for another fifteen minutes.

0.2 M Ammonium Carbonate Solution was added drop by drop to the solution to form precipitation and then filtration was done using a Wattman 41 filter paper.

The filter paper was allowed to dry overnight and powder of $\text{Al}_2\text{O}_3 - 10 \text{LaAl}_{11}\text{O}_{18}$ was collected.

The ultrasonication was done using Ultrasonic Vibratometer.

3.2.4 $\text{Al}_2\text{O}_3 - 40 \text{LaAl}_{11}\text{O}_{18}$ POWDER

1.92 g of Alumina powder was taken in a beaker (say beaker 1) containing distilled water. 0.05 wt% Darvan was also added to form stable solution. The solution was put in ultrasonication for fifteen minutes.

1.81 grams of Lanthanum Oxide powder was taken in a butter paper and was put in a beaker (say beaker 2) containing required amount of distilled water. 2.10 grams of Nitric Acid was added to form Lanthanum Nitrate. The solution was stirred continuously and heated for fifteen minutes.

45.97 grams of Aluminium Nitrate was weighed and put in beaker 2. The solution was again stirred and heated for another fifteen minutes.

Both the solutions were mixed and the solution was reheated for fifteen minutes followed by ultrasonication for another fifteen minutes.

0.2 M Ammonium Carbonate Solution was added drop by drop to the solution to form precipitation and then filtration was done using a Wattman 41 filter paper.

The filter paper was allowed to dry overnight and powder of $\text{Al}_2\text{O}_3 - 10 \text{LaAl}_{11}\text{O}_{18}$ was collected.

The ultrasonication was done using Ultrasonic Vibratometer.

The powders were then weighed and pellets of 0.7 g for each composition were made by applying 4 Ton pressure for 120 seconds. The pellets were then sintered upto 1650°C in a chamber furnace. The soaking time for pellets was 4 hours. The Dry weight, Suspended Weight and Soaked Weight for each pellet was taken and the Bulk Density, Aparent Porosity for each pellet was calculated using the formula

$$\text{BD} = (\text{Dry Wt}) / (\text{Soaked Wt} - \text{Suspended Wt})$$

$$\text{AP} = (\text{Soaked Wt} - \text{Dry Wt}) / (\text{Soaked Wt} - \text{Suspended Wt})$$

The strength of each pellet was then measured using the formula:

$$S = (2*P)/(\pi * D * t)$$

Where P is the load applied.

D is the diameter

t is the thickness.

CHAPTER 4:

Results and Discussion

This section contains all the datas including zeta potential of different aqueous alumina solution, bulk densities, aparent porosities and strengths of pellets with different LHA content in volume percentage.

4.1 Zeta Potential without addition of Electrolyte/Dispersant

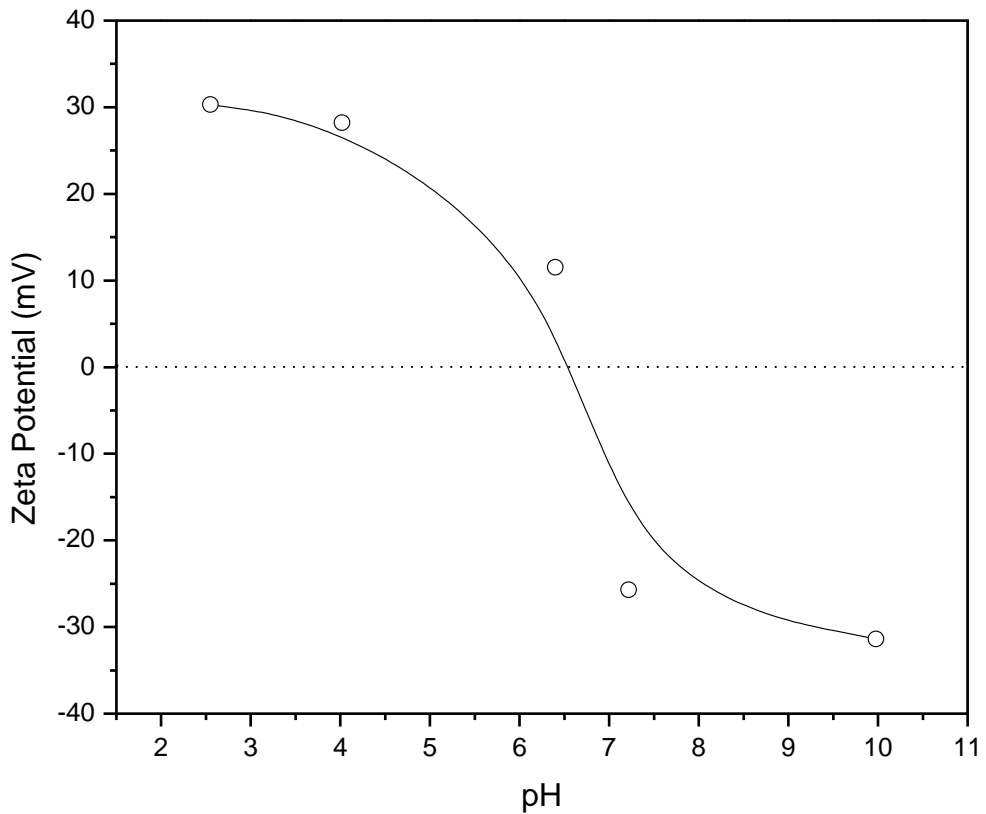


Fig 4.1 shows Zeta Potential v/s pH curve for an aqueous alumina slurry without any addition of electrolyte or dispersant.

The Iso Electric Point from the graph was found to be at pH

4.2 Zeta Potential with addition of Dispersant

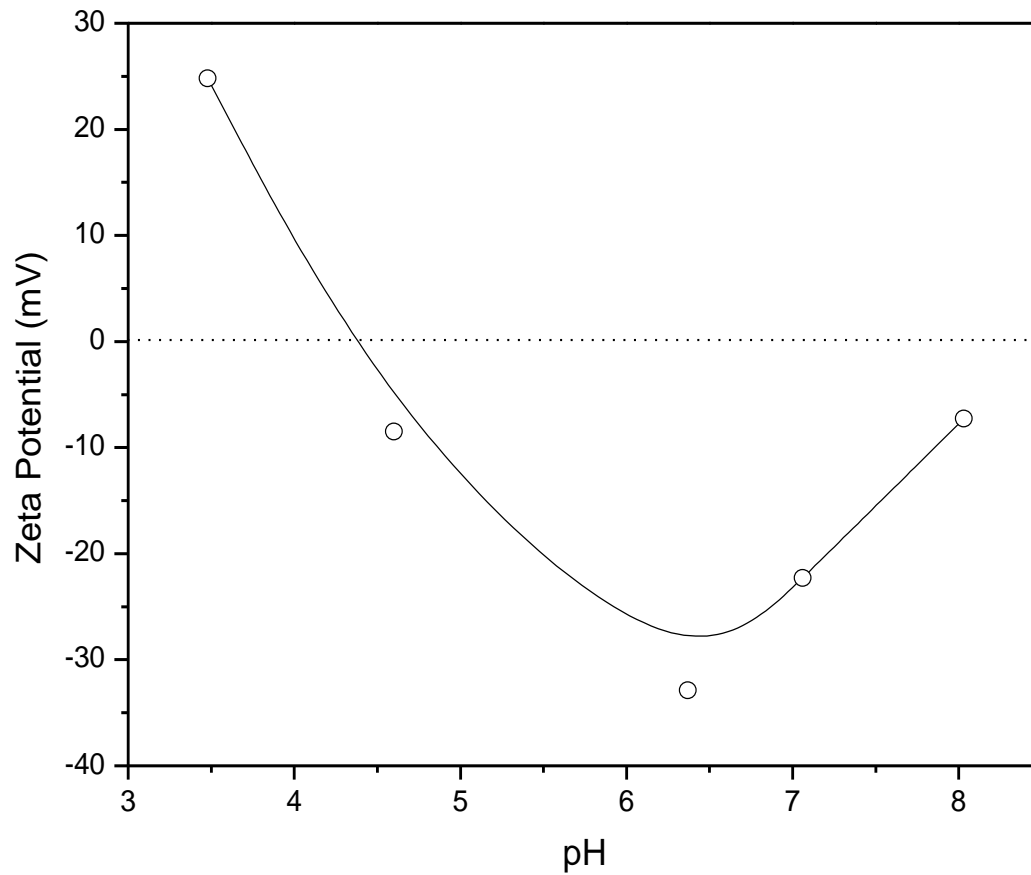


Fig 4.2 shows Zeta Potential v/s pH curve for an aqueous alumina slurry with addition of 0.04 wt. % tri-ammonium cytrate.

More stable solution was observed after addition of a dispersant. The dispersant used was tri-ammonium cytrate. The Zeta Potential increased and hence more stable slurry can be obtained by addition of a dispersant.

4.3 Zeta Potential with addition of Electrolyte

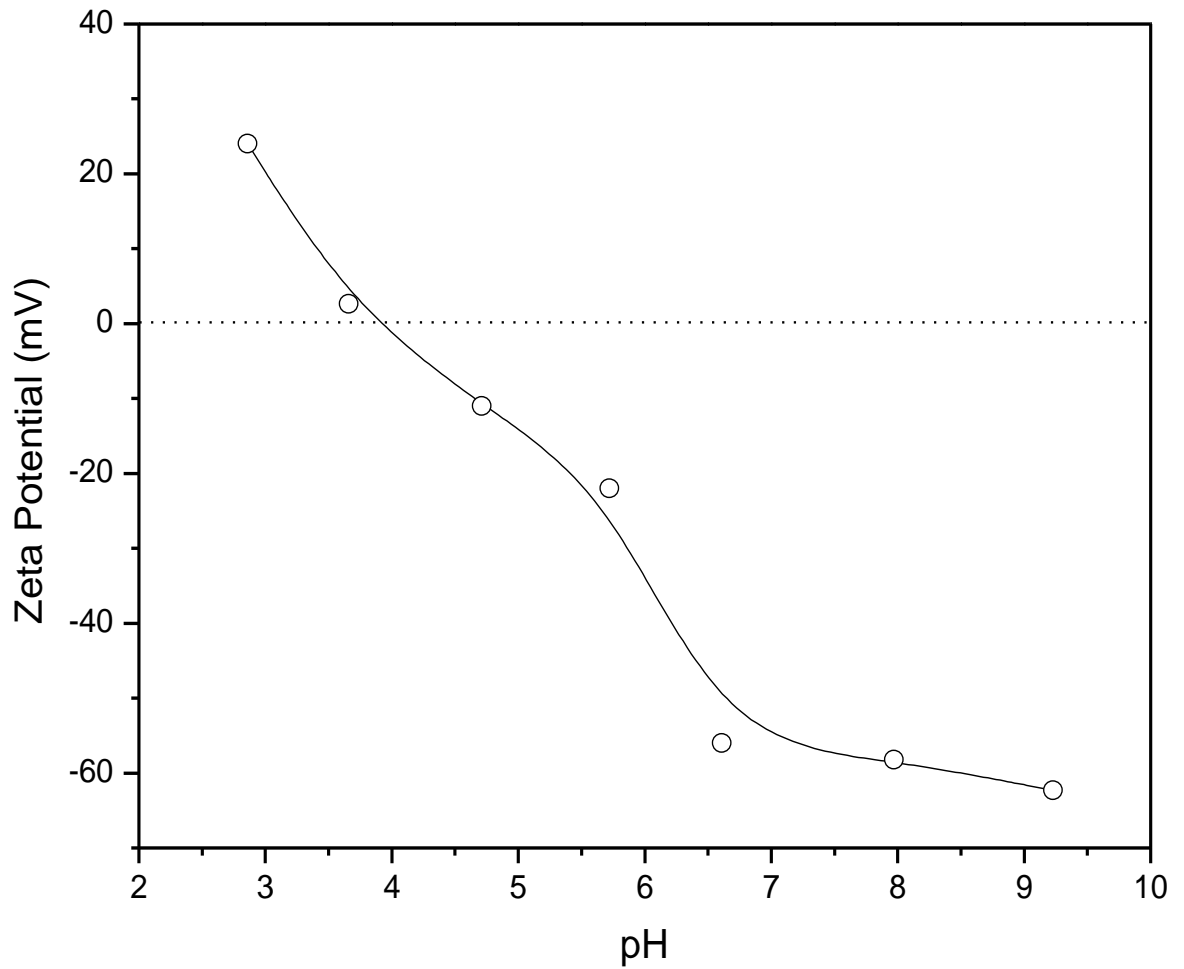


Fig 4.3 shows Zeta Potential v/s pH curve for an aqueous alumina slurry with addition of 0.035wt. % Darvan.

Much better stable solution was observed after addition of an electrolyte. The electrolyte used was Darvan. The Zeta Potential upto 62.3 mV was observed and hence stable slurry can be obtained by addition of a electrolyte.

4.4 Table I

Composition	Dry Wt. (in grams)	Suspended Wt. (in grams)	Soaked Wt. (in grams)	Bulk Density (in g/cc)	Aparent Porosity (in %age)	Strength (in Mpa/mm ³)
Al ₂ O ₃ - 10LaAl ₁₁ O ₁₈	0.6293	0.4682	0.6757	3.03	22	8.88
Al ₂ O ₃ - 20LaAl ₁₁ O ₁₈	0.6245	0.4655	0.6640	3.14	19.89	12.42
Al ₂ O ₃ - 40LaAl ₁₁ O ₁₈	0.5351	0.4001	0.5656	3.23	18.4	13.50
Al ₂ O ₃ - 80LaAl ₁₁ O ₁₈	0.6172	0.4595	0.6415	3.39	12.82	17.36

Fig 4.4 showing the dry wt., suspended wt., soaked wt., bulk density, aparent porosity and strength of pellets with different composition.

4.5 Bulk Density plot for different composition of LHA(Graph I)

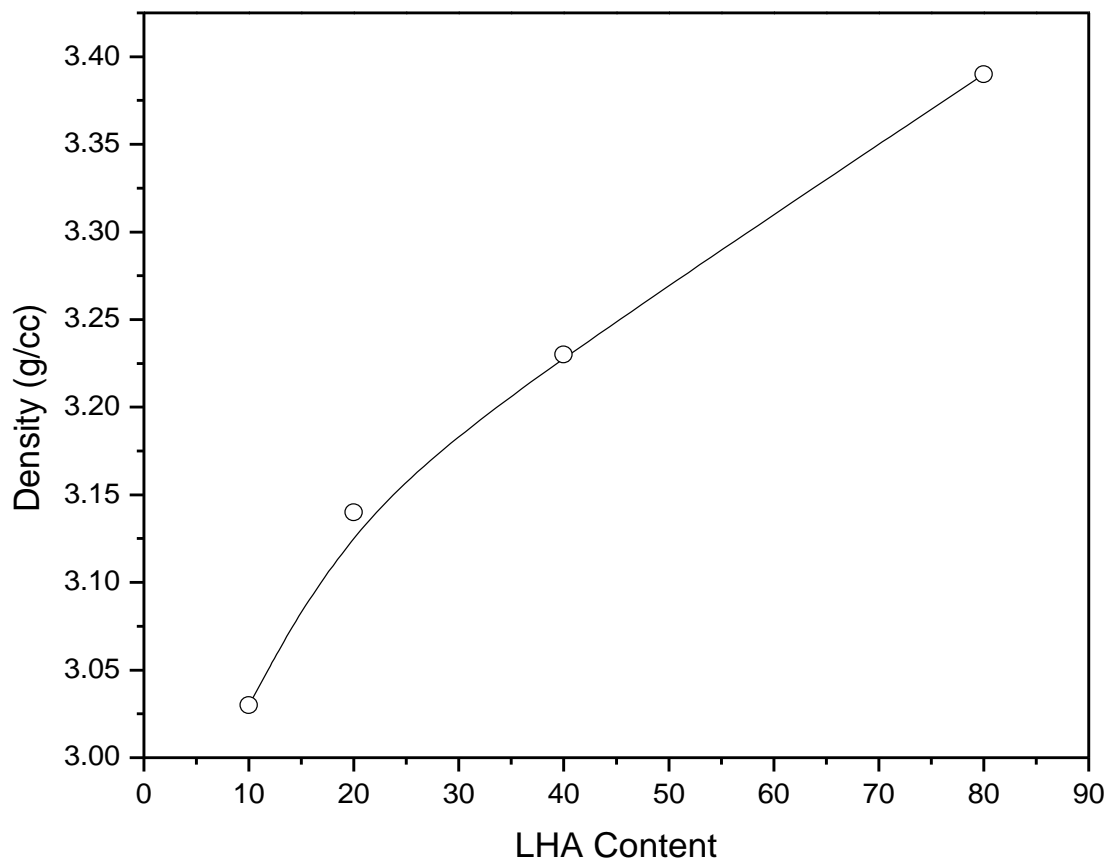


Fig 4.5 showing the bulk density curve obtained for pellets of different composition.

4.6 Bulk Density plot for different composition of LHA(Graph II)

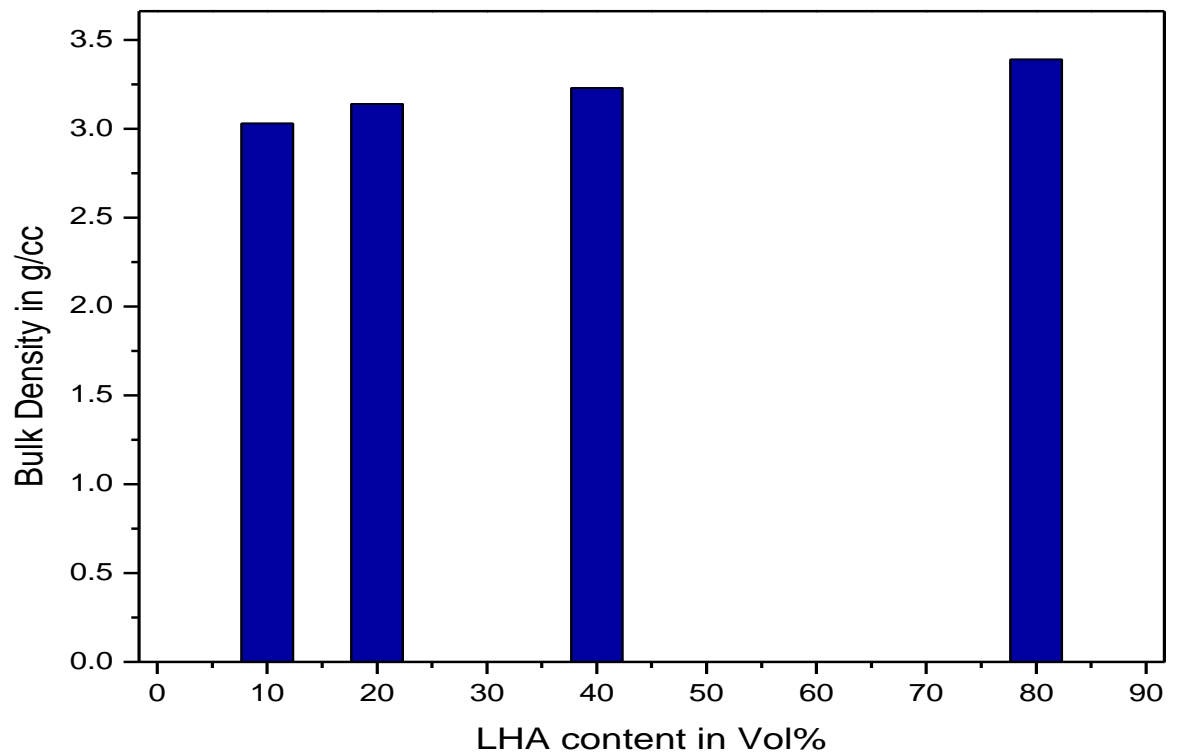


Fig 4.6 showing the bulk density bar for different pellets with composition containing 10 vol% , 20 vol % , 40 vol % and 80 vol% LHA.

Maximum bulk density of 3.39 was obtained for pellet with 80 vol % LHA. The bulk density increased with increase in vol % of LHA content.

4.7 Aparent Porosity plot for different composition of LHA(Graph I)

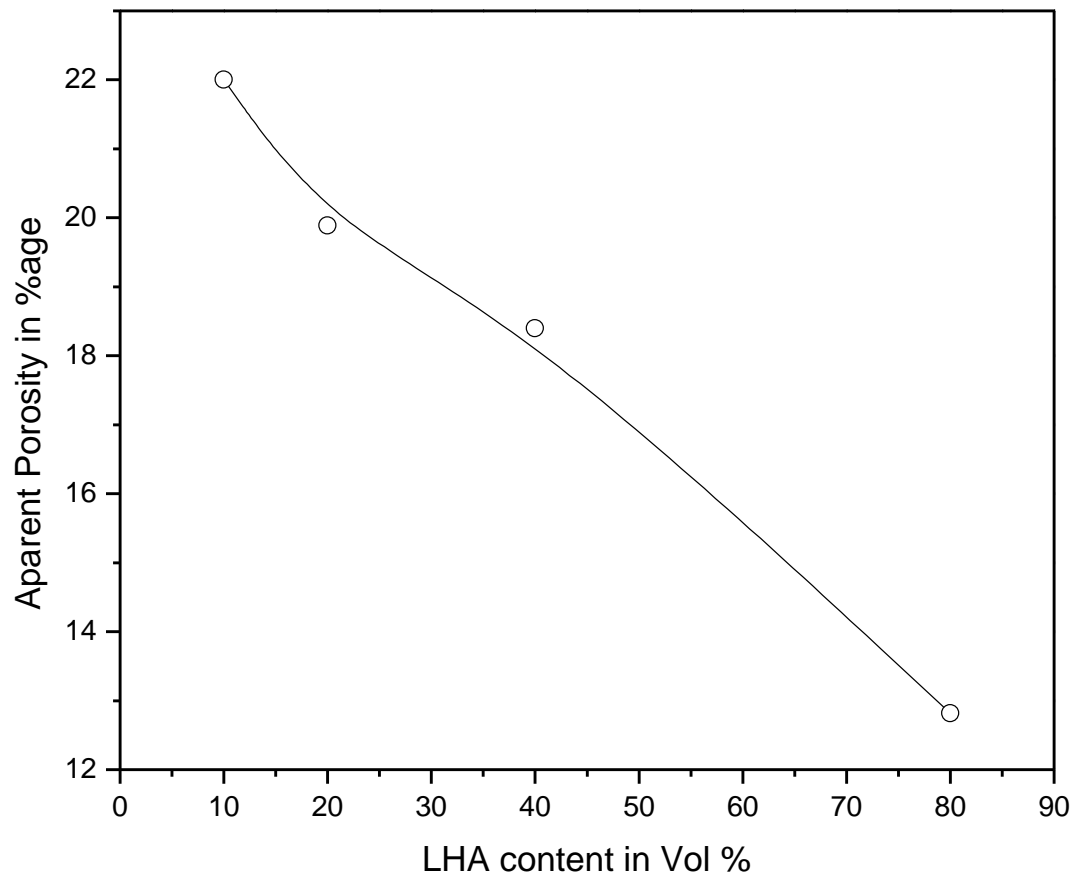


Fig 4.7 showing the aparent porosity curve obtained for pellets of different composition.

4.8 Aparent Porosity plot for different composition of LHA(Graph II)

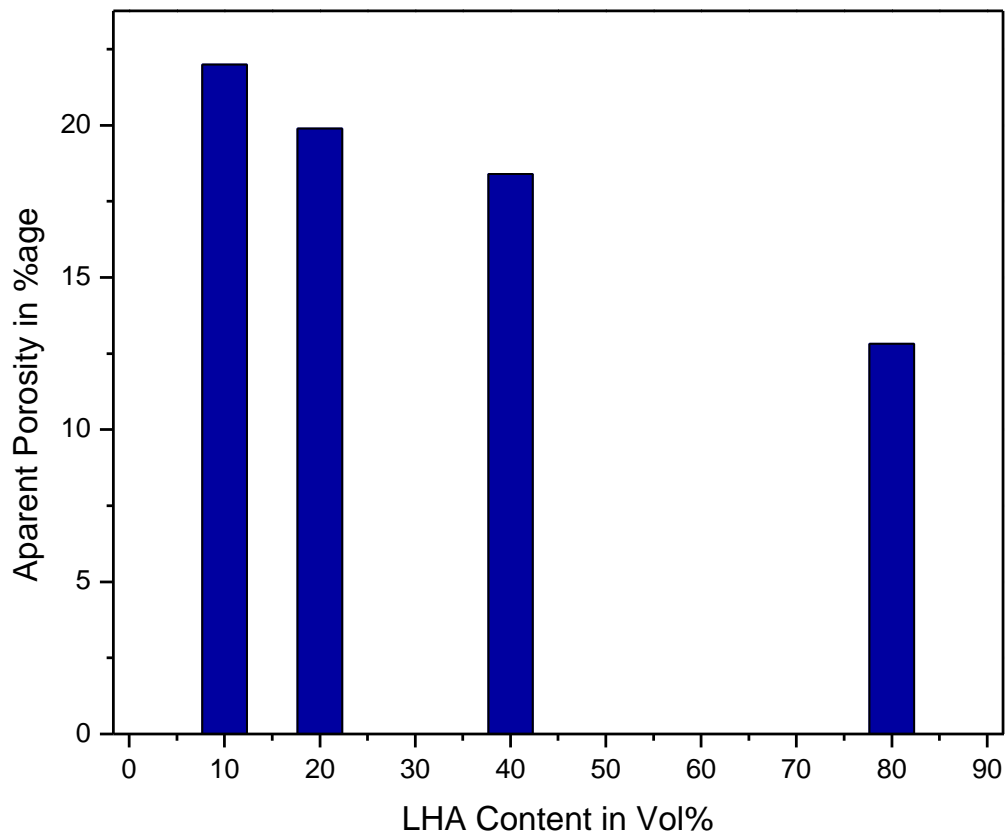


Fig 4.8 showing the aparent porosity bar for different pellets with composition containing 10 vol% , 20 vol % , 40 vol % and 80 vol% LHA.

Maximum aparent density of 22% was obtained for pellet with 10 vol % LHA. The aparent porosity decreased with increase in vol % of LHA content.

4.9 Bar Chart for Strength of Pellets for different composition of LHA

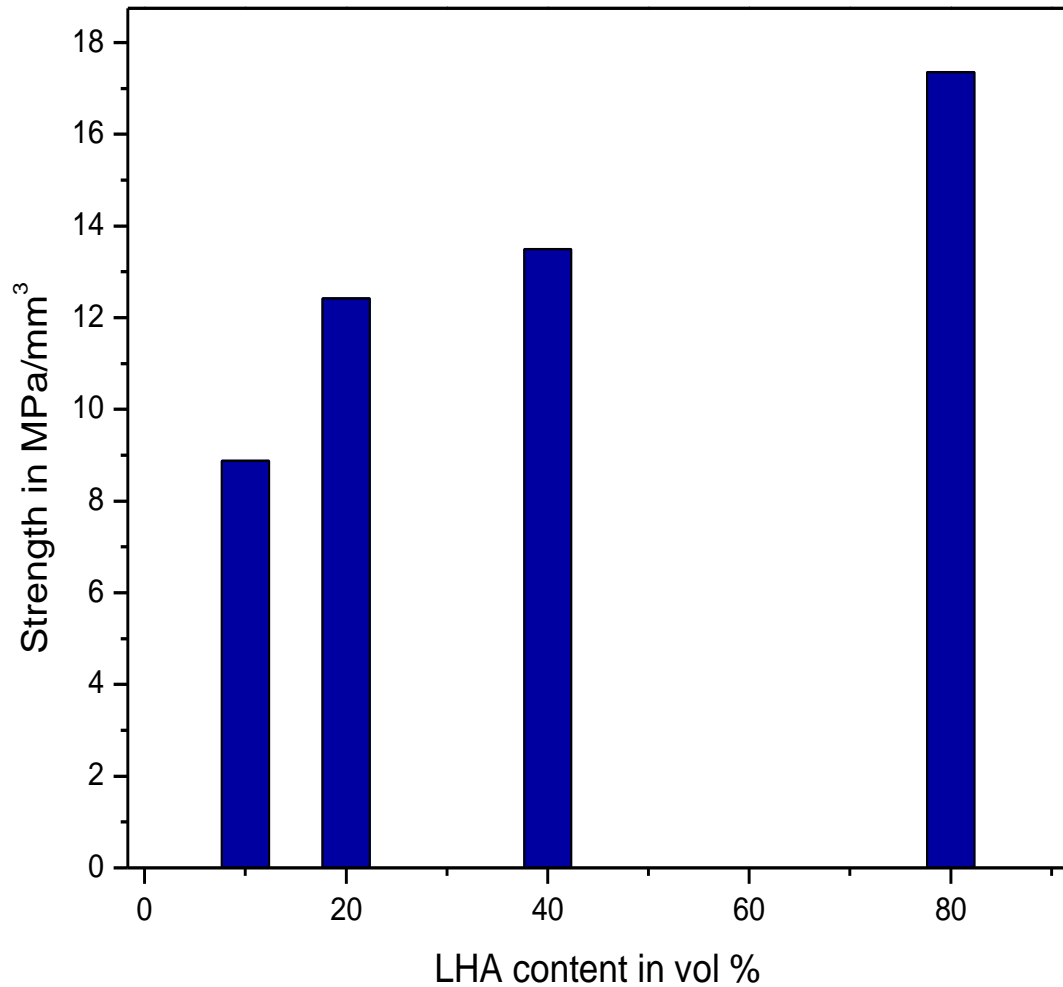


Fig 4.9 showing the strength bar for different pellets with composition containing 10 vol% , 20 vol % , 40 vol % and 80 vol% LHA.

Maximum strength of 17.36 MPa was observed for pellet with composition of 80 vol% LHA.

The strength of pellets increased with increase in vol % of LHA.

4.10 Strength Curve of Pellets for different composition of LHA

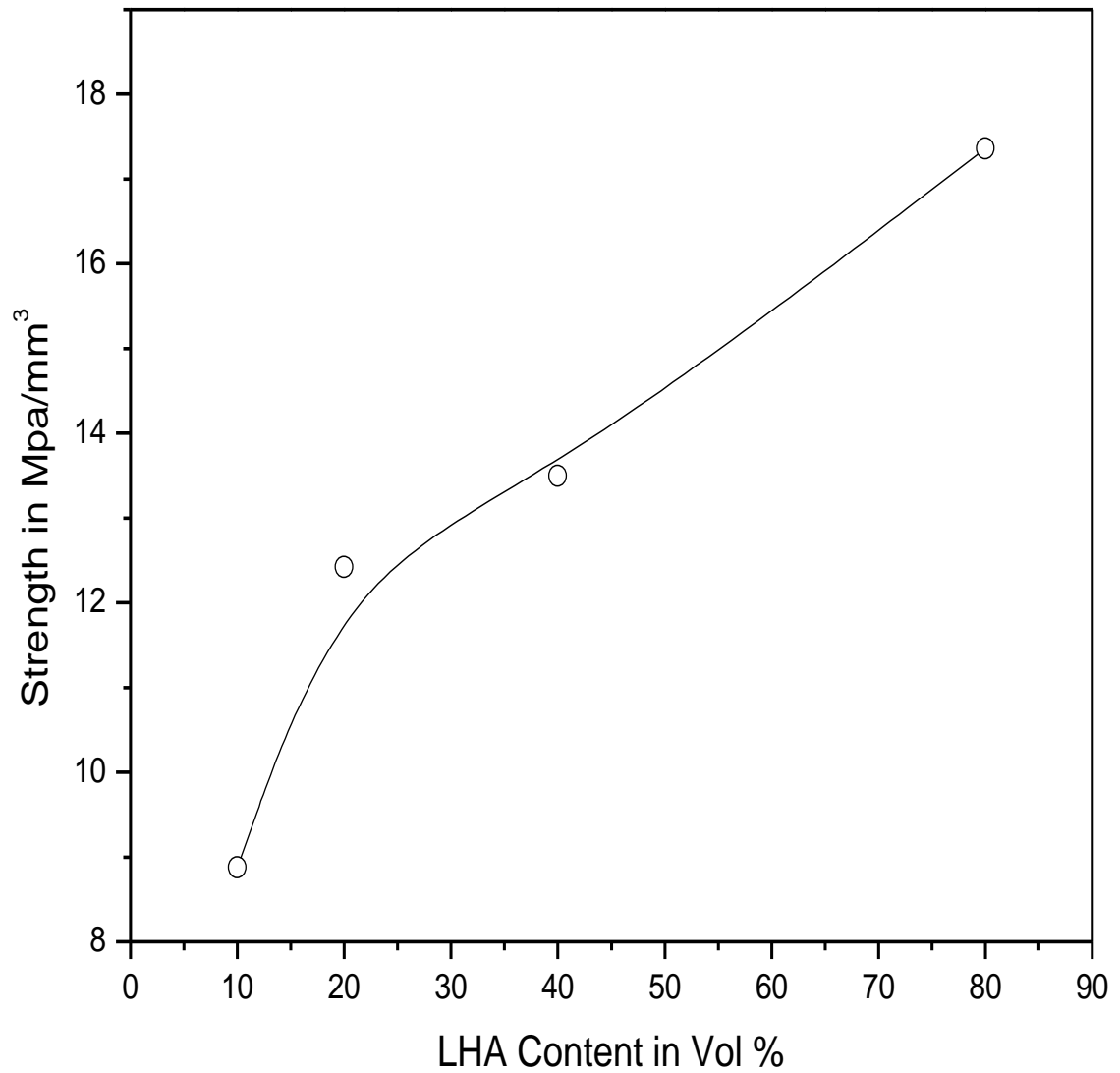


Fig 4.10 showing the strength curve for different pellets with composition containing 10 vol% , 20 vol % , 40 vol % and 80 vol% LHA.

Maximum strength of 17.36 MPa was observed for pellet with composition of 80 vol% LHA.

The strength of pellets increased with increase in vol % of LHA.

5. CONCLUSION

Effect of pH on aqueous alumina slurry was studied. A comparison of Darvan and tri-ammonium Citrate as an electrolyte/dispersant was done and Darvan was chosen as an electrolyte for preparation of aqueous alumina slurry.

Pellets of four different compositions ranging from 10 to 80 vol % of Lanthanum Hexaaluminate were prepared. Sintering of the pellets was done at 1650°C with soaking time of 4 hours. The bulk density, aparent porosity and strength were compared after calculation of dry weight, suspended weight and soaked weight. The results revealed that bulk density increased with increasing vol % of Lanthanum Hexaaluminate and aparent porosity decreased with increasing vol % of Lanthanum Hexaaluminate. The strength also increased with increasing vol % of Lanthanum Hexaaluminate.

6. REFERENCES

1. S. Baklouti, C. Pagnoux, T. Chartier & J. F. Baumard, Processing of Aqueous α - Al_2O_3 , α - SiO_2 and α - SiC Suspensions with Polyelectrolytes, *Journal of the European Ceramic Society* 17 (1997) 1387-1392.
2. R. Ramachandra Rao, H. N. Roopa and T. S. Kannan, Dispersion, Slip Casting and Reaction Nitridation of Silicon-Silicon Carbide Mixtures, *Journal of the European Ceramic Society* 19 (1999) 2145-2153.
3. Xinwen Zhu, Dongliang Jiang, Shouhong Tan, The control of slurry rheology in the processing of reticulated porous ceramics, *Materials Research Bulletin* 37(2002) 541-553.
4. Pang Xueman, Xu Mingxia, Liang Hui, Li Xiaolei, Ji Huiming, Rheological properties and thixotropy model of concentrated aqueous silicon slurry for gel casting, *Colloids and Surfaces A: Physicochem. Eng. Aspects* 317 (2008) 136–145.
5. F.S. Ortega, R.H.R. Castro, D. Gouvea , V.C. Pandolfelli, The Rheological Behaviour and Surface Charging of Gelcasting Alumina Suspensions, *Ceramics International* 34 (2008) 237–24.
6. P.C. KAPUR, Thermal Insulations from Rice Husk Ash, an Agricultural Waste, *CERAMURGIA INTERNATIONAL*. Vol. 6. n. 2. 1953.
7. C. Friedrich, R. Gadow, and T. Schirmer, Lanthanum Hexaaluminate – a New Material for Atmospheric Plasma Spraying of Advanced Thermal Barrier Coatings, *JTTEE5* 10:592-598.

8. N. Iyi, Z. Inoue, S. Takekawa and S. Kimura, The crystal structure of lanthanum hexaaluminate, *Journal of Solid State Chemistry* volume 54, Issue 1, August 1984, Pages 70 – 77.
9. R. Gadow and M. Lischka, Lanthanum hexaaluminate — novel thermal barrier coatings for gas turbine applications — materials and process development, *Surface and Coatings Technology*, Volumes 151-152, 1 March 2002, Pages 392-399.
10. Zahra Negahdari, Monika Willert-Porada, Tailoring the microstructure of reaction-sintered alumina/lanthanum hexaaluminate particulate composites, *Journal of the European Ceramic Society* 30 (2010) 1381–1389.
11. Krenkel W, Naslain R, Schneider H. *High Temperature Ceramic Matrix Composite*. Wiley-VCH; 2001.
12. Wendorff J, Janssen R, Clauss N. Model experiments on pure oxide composites. *Mater Sci Eng A* 1998;**250**:186–93.
13. Becher PF. Microstructural design of toughened ceramics. *J Am Ceram Soc* 1991;**74**(2):255–69.
14. Inagaki Y, Kondo N, Ohji T. High performance porous silicon nitrides. *J Eur Ceram Soc* 2002;**22**:2489–94.
15. Cinibulk MK. Hexaaluminates as a cleavable fibre-matrix interphase: synthesis, texture development, and phase compatibility. *J Eur Ceram Soc* 2000;**20**:569–82.
16. Chen PL, Chen IW. In-situ alumina/aluminate platelet composites. *J Am. Ceram Soc* 1992;**75**(9):2610–2.

17. Gadow R, Lischka M. Lanthanum hexaluminat-novel thermal barrier coatings for gas turbine applications: materials and process development. *Surf Coat Technol* 2002;**151-2**:392–9.
18. Ropp RC, Carroll B. Solid-state kinetics of LaAl₁₁O₁₈. *J Am Ceram Soc* 1980;**63**(7–8):416–9.
19. Jang BK, Kishi T. Fabrication and microstructure of Al₂O₃ matrix composites by in-situ reaction in the Al₂O₃–La₂O₃ system. *J Ceram Soc Jpn* 1998;**106**(8):739–43.
20. Barrera-Solano C, Esquivias L. Effect of preparation conditions on phase formation, densification, and microstructure evolution in La-Al₂O₃/Al₂O₃ composites. *J Am Ceram Soc* 1999;**82**(5):1318–24.
21. Wu YQ, Zhag YF, Huang XX, Li BS, Guo JK. Preparation, sintering and fracture behaviour of Al₂O₃–LaAl₁₁O₁₈ ceramic composites. *J Mater Sci* 2001;**36**:4195–9.
22. Nair J, Nair P, Doesburg EBM, Van Ommen JG, Burggraaf AJ, Mizukami F. Textural stability as a characterisation tool of high temperature catalysts. *Mater Res Innov* 1998;**2**:72–8.
23. Cao XQ, Zhang YF, Zhang JF, Zhong XH, Wang Y, Ma HM, Xu ZH, He LM, Lu F. Failure of the plasma-sprayed coating of lanthanum hexaluminat. *JEur Ceram Soc* 2008;**28**(10):1979–86.
24. Rahaman MN. *Ceramic Processing*. 1st ed. Taylor & Francis Group; 2008
25. Asmi D, Low IM. Self-reinforced Ca-hexaluminat/alumina composites with graded microstructures. *Ceram Int* 2008;**34**(2):311–6.
26. Rahaman MN. *Sintering of Ceramic*. 1st ed. Taylor & Francis Group; 2008.
27. Herring C. Effect of change of scale on sintering phenomena. *J Appl Phys* 1950;**21**:301–3.

28. Yoshida H, Hashimoto S, Yamamoto T. Dopant effect on grain boundary diffusivity in polycrystalline alumina. *Acta Mater* 2005;**53**:433–40.
29. Hazzledine PM. Grain boundary pinning in two-phase materials. *Czech J Phys B* 1988;**38**:431–43.
30. Vishista K, Awaji H, Gnanam FD. Sol–gel synthesis and characterization of alumina-calcium hexaluminate composites. *J Am Ceram Soc* 2005;**88**(5):1175–9.
31. An L, Chan HM, Soni KK. Control of Calcium hexaluminate grain morphology in in-situ toughened ceramic composites. *J Mater Sci* 1996;**31**:3223–9.
32. Kingery WD. *Introduction to Ceramics*. John Wiley & Sons; 1960